Published in final edited form as:
Neuron. 2009 November 25; 64(4): 498–509. doi:10.1016/j.neuron.2009.09.030.

Various signals involved in nociception regulate TRPA1 levels at the plasma membrane

Manuela Schmidt[1], **Adrienne E. Dubin**[1], **Matt J. Petrus**[2], **Taryn J. Earley**[1], and **Ardem Patapoutian**[1,2]

[1] Department of Cell Biology, The Scripps Research Institute, La Jolla, California 92037, USA

[2] Genomics Institute of the Novartis Research Foundation, San Diego, California 92121, USA

Abstract

Transient receptor potential A1 (TRPA1) ion channel senses a variety of noxious stimuli, and is involved in nociception. Many TRPA1 agonists covalently modify the channel and can lead to desensitization. The fate of modified TRPA1 and the mechanism of preserving its response to subsequent stimuli are not understood. Moreover, inflammatory signals sensitize TRPA1 involving protein kinase A (PKA) and phospholipase C (PLC) through unknown means. We show that TRPA1-mediated nocifensive behavior can be sensitized *in vivo* via PKA/PLC signaling and by activating TRPA1 with the ligand mustard oil (MO). Interestingly, both stimuli increased TRPA1 membrane levels *in vitro*. Tetanus toxin attenuated the response to the second of two pulses of MO in neurons, suggesting vesicle-fusion to increase functional surface TRPA1. Capacitance recordings suggest that MO can induce exocytosis. We propose that TRPA1 translocation to the membrane might represent one of the mechanisms controlling TRPA1 functionality upon acute activation or inflammatory signals.

INTRODUCTION

TRPA1 is an essential transduction ion channel expressed in sensory neurons of the dorsal root ganglia (DRG) and trigeminal ganglia (TG), and is involved in acute and inflammatory pain (Bandell et al., 2004; Bautista et al., 2006; Katsura et al., 2006; Kwan et al., 2006; Macpherson et al., 2007; Obata et al., 2005; Story et al., 2003). As a sensor of chemical damage TRPA1 can be activated by surprisingly diverse electrophilic and nonelectrophilic chemicals. Electrophilic TRPA1 agonists, like allyl-isothiocyanate (mustard oil, MO) and cinnamaldehyde, do not share structural similarity, but exert their activity through covalent modification of cysteine residues within the intracellular N-terminus of TRPA1 (Hinman et al., 2006; Macpherson et al., 2007). Given that the half-life of isothiocyanate-cysteine

Corresponding Author: Dr. Ardem Patapoutian, Department of Cell Biology, The Scripps Research Institute, ICND, 10550 N Torrey Pines Road, La Jolla, California 92037, USA, Phone: (858) 784-9879, Fax: (858) 784-9860, apatapou@gnf.org.

AUTHOR CONTRIBUTIONS

M.S. and A.P. planned the project. M.S. designed experiments and carried out calcium imaging, live-labeling and immunostainings. M.J.P. performed behavioral experiments. A.E.D. designed and carried out capacitance recordings and helped write the manuscript. T.J.E. provided neuronal cultures. M.S. and A.P. wrote the manuscript.

SUPPLEMENTAL DATA

Supplemental data include Supplemental Experimental Procedures and five figures.

complexes is in the order of 1 hour, this unique mode of activation imposes a substantial problem to signal termination, as the response of TRPA1 to electrophilic agonists would be predicted to last far beyond the stimulus duration (Conaway et al., 2001). Desensitization (tachyphylaxis) of TRPA1 in response to chemical agonists offers a short-term solution to this problem (Wang et al., 2008b). However, maintenance of the sensitivity of nociceptive neurons to subsequent stimulation by TRPA1 agonists is critical, and how this is accomplished is not known.

In addition to its role in acute nociception, TRPA1 has been implicated in sensing inflammatory signals. Tissue damage and inflammation cause physiological changes to sensory neurons involving reduced threshold and enhanced responsiveness (peripheral sensitization). A variety of signals including chemokines, growth factors, kinins, proteases and various kinases have been implicated in inducing peripheral sensitization (Hucho and Levine, 2007). The resulting hyperalgesia (exaggerated pain response) and allodynia (pain response to innocuous stimuli) is thought to contribute to the etiology of chronic pain syndromes. Recently, signaling pathways leading to TRPA1 sensitization or potentiation have been reported (Dai et al., 2007; Wang et al., 2008a). These studies suggest sensitization of TRPA1-mediated nocifensive behavior upon injection of bradykinin and activators of proteinase-activated receptor (PAR) 2, respectively. Furthermore, *in vitro,* electrophysiological recordings on DRG neurons imply the involvement of protein kinase A (PKA) and phospholipase C (PLC) signaling in potentiating MO-induced TRPA1 currents (Dai et al., 2007; Wang et al., 2008a); however, the molecular mechanisms remain to be elucidated.

The function of a variety of ion channels and receptors is known to be regulated by their constitutive or regulated trafficking. In the central nervous system, the tight regulation of AMPA receptor cycling between plasma membrane and intracellular compartments underlies synaptic plasticity (Malenka, 2003; Shepherd and Huganir, 2007). Moreover, there is ample evidence that long-lasting modulation of nociceptive receptor surface expression is associated with differentially altered trafficking. For example, sensitization of trigeminal neurons by calcitonin gene-related peptide (CGRP) increases currents through ATP-activated purinergic $P2X_3$ receptors by enhancing their translocation to the membrane (Fabbretti et al., 2006). Similarly, sensitization of TRPV1 channels by nerve growth factor (NGF) partly involves TRPV1 membrane trafficking (Ji et al., 2002; Zhang et al., 2005). On the other hand, several studies have shown that cannabinoid-induced internalization of type 1 cannabinoid receptor (CB1) contributes to tolerance (Tappe-Theodor et al., 2007). A different mechanism seems to account for morphine-induced tolerance, where receptor internalization and recycling to the cell surface is required to render the receptors competent after morphine binding (Zhang et al., 2006). Similar mechanisms might account for the unique activation characteristics of electrophilic agonists on TRPA1 as well as TRPA1 sensitization. Despite the importance of TRPA1 in transducing noxious stimuli, and numerous studies describing various mechanisms of TRPA1 activation, little is known about TRPA1 membrane trafficking and the regulation of channel availability at the cell surface.

In this study, we set out to address the regulation of TRPA1 membrane levels using a combination of immunostaining, live-labeling, calcium imaging and electrophysiology. Our data suggest that different stimuli converge to recruit functional TRPA1 channels to the plasma membrane, uncovering a potential molecular mechanism for the involvement of TRPA1 in sensing acute tissue damage and in peripheral sensitization.

RESULTS

TRPA1-mediated pain responses are sensitized *in vivo*

The role of TRPA1 in sensing acute damage is well-established. However, less is known about its role in inflammation. Recently, it has been demonstrated that protein kinase A (PKA) and phospholipase C (PLC) signaling pathways sensitize mustard oil (MO)-induced TRPA1 currents *in vitro* (Dai et al., 2007; Wang et al., 2008a). We initially tested whether the TRPA1 sensitization observed *in vitro* is of physiological relevance *in vivo*. Injection of a combination of forskolin (FSK, which activates adenylyl cyclase) and m-3m3FBS (an activator of PLC-signaling) into the left hindpaw of mice did not evoke obvious nocifensive behaviors. Ten minutes later, a relatively low amount of MO (1 mM) was injected, and animals were observed for pain behaviors (nocifensive response). Interestingly, the duration of MO-induced nocifensive responses was significantly increased upon pretreatment with FSK and m-3m3FBS compared to vehicle (Figure 1A). We then tested whether activation of either PKA or PLC signaling sensitized TRPA1 channels *in vivo*. Indeed, pretreatment with higher concentrations of FSK sensitized nocifensive responses to MO. Interestingly, FSK at this concentration did not affect thermal hyperalgesia, arguing for some specificity (data not shown). We also assayed m-3m3FBS alone and observed a trend toward sensitization, but no statistical significance (Figure 1B). We were not able to increase the concentration of m-3m3FBS due to unspecific effects of the vehicle (EtOH) at higher concentrations (> 12% EtOH caused pain and could not be used in our assay). Our results suggest that sensitization by PKA and PLC activators is functionally relevant for TRPA1 physiology.

In a related set of experiments, the *in vivo* consequence of repeated MO application was tested. Under some recording conditions (e.g. whole cell in presence of calcium), MO causes severe tachyphylaxis of TRPA1, such that repeated stimuli evoke highly diminished responses (Dai et al., 2007; Ruparel et al., 2008; Wang et al., 2008a). The mechanism for this is not completely understood, but involves calcium (in inside out patches without calcium this desensitization is not observed) (Macpherson et al., 2007; Wang et al., 2008b). We assayed nocifensive behavior to consecutive application of MO to the same region of the hindpaw and asked whether a second response could be elicited. Although the two injections were directed to the same location in the hindpaw, we cannot say with certainty that the same neuronal endings were exposed. Mice responded to the first injection of MO with only minor nocifensive behavior (Figure 1C). Nocifensive responses were strongly enhanced upon the second injection of MO. This effect was specific to injection of MO, as injection of vehicle resulted in significantly reduced nocifensive behavior (Figure 1C). Interestingly, the observed sensitization of nocifensive responses to a second MO challenge was significantly stronger than responses to a single injection of twice the amount of MO (Figure 1C). To control for potential olfactory-related effects of the pungent odor of MO in our paradigm we assayed nocifensive behavior to consecutive injections of MO or vehicle in the presence of a pad containing the amount of MO that we normally injected (10 μl of 10 mM MO). Adding this MO-containing pad into the test cage of both experimental and control groups during the evaluation of the second injection did not influence the experimental outcome (data not shown). From this set of data we conclude that the odor of MO does not influence the nocifensive behavior of either group. Taken together, these observations suggest that TRPA1 channels can be sensitized *in vivo* by either inflammatory signals or electrophilic activators of TRPA1. To gain insight into mechanisms of dynamic regulation of TRPA1 function, we focused on creating tools to study TRPA1 localization.

Live-labeling of the surface population of TRPA1 channels in HEK cells

As fluorescent-tagging of TRPA1 (GFP fusions to N- and C-termini of TRPA1 as well as a random insertion approach) did not yield functional channels. In an effort to visualize TRPA1

channels at the surface of live cells, we generated peptide antibodies directed against two epitopes (AbE1, AbE3) in extracellular loops one and three of murine TRPA1 (mTRPA1). Antisera-specificity was determined by indirect immunohistochemistry on cryosections of trigeminal ganglia (TG) from wildtype and TRPA1-deficient mice (Figure 2A). TRPA1 staining was observed in roughly 8 % of wildtype neurons (n = 3516 from 4 mice, see also results below), while no detectable labeling was present in neurons from *Trpa1*-deficient mice prepared in parallel. Both antibodies gave similar results. We expect that neurons with relatively high TRPA1 expression are labeled as previous studies using *in situ* hybridization reported 3.6 % to 36.5 % of TG neurons being positive for *Trpa1* mRNA (Diogenes et al., 2007; Nagata et al., 2005; Story et al., 2003). Co-labeling with CGRP, a marker for nociceptive neurons, revealed that TRPA1-positive neurons are also positive for CGRP (Figure 2B) as described in earlier reports (Bautista et al., 2005; Story et al., 2003).

We next attempted to detect the surface population of TRPA1 channels in Human Embryonic Kidney (HEK) 293T cells transiently transfected with a murine *Trpa1*-MYC/His construct (Macpherson et al., 2007). HEK cells were incubated with AbE1 at 37 °C for 10 minutes, washed to remove unbound antibodies and treated with Fab fragments conjugated to Alexa Fluor 488 at room temperature for another 10 minutes. Figure 2C shows representative z-stacks of HEK cells live-labeled for surface TRPA1 (green). The surface staining exhibited a clear punctate pattern. This was distinct from the signal obtained when visualizing the total population of TRPA1-MYC with a MYC-antibody after fixation and permeabilization (blue). A wheat germ agglutinin (WGA) Alexa Fluor 555 conjugate was used to delineate membranes (red). Importantly, surface labeling was specific for TRPA1, as only TRPA1-MYC-expressing cells were stained. Loss of TRPA1-membrane signal upon acid stripping (Beattie et al., 2000) indicates that the observed staining indeed reflected surface labeling (Figure S1).

Regulation of membrane levels and functionality of TRPA1 in response to PKA/PLC activators

Having established live-labeling of surface TRPA1, we tested whether activation of PKA and PLC pathways in HEK cells expressing TRPA1 might serve as a molecular correlate of the sensitization of TRPA1 observed *in vivo*. Remarkably, application of FSK and m-3m3FBS significantly increased the levels of TRPA1 at the membrane (Figures 3A,B). Figure 3A shows representative images obtained after FSK, m-3m3FBS application compared to vehicle. For quantitation of this effect, the mean fluorescence intensity of TRPA1 surface label was measured and FSK, m-3m3FBS-treated cells were compared with vehicle-treated cells (Figure 3B). Application of either substance alone at these concentrations did not alter TRPA1 surface label. However, similar to our behavioral results (Figure 1B), application of higher concentrations of FSK or m-3m3FBS resulted in an increase of TRPA1 surface labeling (Figures 3C,D), albeit not to the same extent as the combination of both compounds at lower concentrations (Figure 3A). A similar, potentially additive effect of FSK and m-3m3FBS on TRPA1-mediated currents has been reported by Wang and colleagues (Wang et al., 2008a). Our results indicate for the first time that TRPA1 channels might be actively translocated to the membrane. Next, we tested whether the newly recruited channels might be functional. We performed fluorometric imaging plate reader (FLIPR)-based calcium imaging of transfected HEK cells. Of note, m-3m3FBS induced calcium influx in TRPA1-expressing HEK cells (Bandell et al., 2004) likely due to activation of PLC pathways, as this activation was strongly attenuated by the PLC inhibitor edelfosine (data not shown). For this reason, we focused on FSK in FLIPR-based calcium imaging. Incubation of TRPA1-expressing HEK cells with FSK 7 minutes before addition of low concentrations of MO potentiated TRPA1-mediated responses (Figure 3E). We also tested whether endogenous TRPA1 channels in cultured sensory neurons are sensitized by PKA and PLC signaling pathways. In contrast to our studies on overexpressed TRPA1 in HEK cells, cultured sensory neurons did not exhibit m-3m3FBS-induced calcium

influx (Figure S2) and we were able to test for sensitization of MO-responses using a combination of FSK and m-3m3FBS. In accordance with our behavioral data and TRPA1 live-labeling in HEK cells, we observed an increase in the number of responding neurons to MO after pretreatment with FSK and m-3m3FBS (Figure 3F and Figure S2). In summary, our data suggest that TRPA1 channels actively translocate to the membrane and that these channels might be functional.

Activation of TRPA1 by MO increases TRPA1 surface labeling

We next sought to explore whether TRPA1 activation by its specific agonist MO could increase TRPA1 at the membrane. Indeed, incubation of TRPA1-espressing HEK cells with MO resulted in a pronounced increase in surface labeling compared to incubation with vehicle (Figures 4A,B). We then addressed the mechanism(s) by which TRPA1 surface levels were increased. First, we examined the potential involvement of PKA and PLC signaling and pre-treated transfected HEK cells with FSK and m-3m3FBS followed by exposure to MO. We did not detect any further enhancement of TRPA1 surface levels (Figure 4B). On the other hand, co-application of a PKA-inhibitor (H89) and the PLC inhibitor edelfosine (ET) attenuated the MO-induced increase in TRPA1 surface staining (Figure 4C). Basal levels of TRPA1 were unaffected by H89 and ET (Figure 4C) and neither H89 nor ET blocked MO-mediated TRPA1 activity. These results suggest that TRPA1 activation enhances TRPA1 expression at the membrane, and that this is at least partly dependent on activation of PKA/PLC. One of the consequences of MO-induced TRPA1 activation is a rise of intracellular calcium since TRPA1 is a non-selective cation channel. We therefore tested the influence of calcium on TRPA1 surface levels. First, MO was applied in calcium-free solution, which allows for channel activity, but not calcium influx. Under these calcium-free conditions, MO did not affect TRPA1 surface labeling (Figure 4D). This demonstrates that calcium influx through TRPA1 is required for MO-induced increased surface levels. Of note, this result argues against the possibilities that i) the observed effects on TRPA1 surface levels might simply be due to the reactive nature of MO (Macpherson et al., 2007) and independent of its ability to activate TRPA1, or ii) binding of TRPA1 antibodies might be enhanced upon TRPA1 activation. As TRPA1 is highly co-expressed with TRPV1 in sensory neurons (Story et al., 2003), we further asked whether activation of TRPV1 and its accompanying calcium influx increased TRPA1 membrane expression. Rat TRPV1 was co-expressed with TRPA1 in HEK cells and activated by capsaicin (CAPS). Interestingly, TRPA1 surface staining increased upon CAPS-treatment (Figure 4E and Figure S3A), while TRPV1 levels were unchanged (Figures S3A,B). Our data on TRPV1 are in accordance with a previous report showing that TRPV1 surface expression is not affected by CAPS (Bao et al., 2003). We then investigated whether a general rise of intracellular calcium could cause an increase in surface levels of TRPA1. Addition of ATP to TRPA1-expressing cells to cause calcium release from intracellular stores via endogenous P2Y receptor activation did not alter the abundance of TRPA1 channels at the membrane compared to vehicle controls (Figure 4F).

Taken together, we propose that localized calcium influx upon TRPA1 and TRPV1 activation increases surface expression of TRPA1 while a more general elevation of intracellular calcium does not. These data are consistent with the notion that localized calcium changes in microdomains form the basis for many cellular processes (Oheim et al., 2006).

Acute upregulation of endogenous TRPA1 in sensory neurons

Next, we investigated whether endogenous TRPA1 in sensory neurons exhibited a similar augmentation of surface levels upon MO-induced channel activity. Several reports showed enhanced expression of TRPA1 after application of various painful stimuli (Ji et al., 2008; Obata et al., 2005). These studies investigated long-term effects on trpa1 mRNA levels. Nonetheless, our data using heterologously expressed TRPA1 suggested an acute regulation

of TRPA1 protein. To test this *in situ*, we incubated explants of trigeminal ganglia with MO, obtained cryosections, and stained for TRPA1. MO-treated explants exhibited significantly greater numbers of TRPA1-positive neurons when compared to vehicle-treated controls (Figure 5A,B). In contrast, staining for the nociceptive marker peripherin was unchanged (data not shown). This result is in accordance with our experiments in HEK cells showing that activation of TRPA1 causes its rapid upregulation.

Since immunohistochemistry on fixed and permeabilized tissue is not suited for differentiating among effects on translation, posttranslational modifications, or trafficking of TRPA1, we performed live-labeling of endogenous TRPA1 channels in cultured DRG neurons. We obtained a punctate pattern of surface staining similar to that observed with transfected HEK cells; however, the efficiency of TRPA1 live-labeling was very low in cultured DRG neurons. Only ~1 % of cultured neurons appeared TRPA1-positive, in contrast to ~29 % of neurons responding to MO in ratiometric calcium imaging experiments (Bautista et al., 2006) (see results below). This discrepancy is likely due to limited sensitivity of our antibodies to the low levels of endogenous TRPA1. Nevertheless, the observed surface staining was specific for TRPA1, as neurons derived from *Trpa1*-deficient animals were devoid of signal (data not shown). In accordance with the data presented above, addition of MO to these neurons resulted in significant recruitment of TRPA1 channels to the plasma membrane (Figure 5C,D).

Evidence for vesicle-mediated membrane translocation of TRPA1

Collectively, we show here that heterologously expressed and native TRPA1 levels at the cell surface can be increased in response to various signals, including TRPA1 activity. Furthermore, we demonstrate that calcium is required for the MO-induced increase of TRPA1 levels in HEK cells. An increase in surface receptors could be accomplished by two different processes: attenuation of constitutive endocytosis/retrieval of TRPA1 channels from the membrane, or induced delivery and insertion of TRPA1 channels into the membrane. These two mechanisms are not mutually exclusive, and a combination of both is possible. To elucidate whether increased TRPA1 membrane levels are at least partly due to exocytotic insertion of TRPA1, sensory neurons were incubated with tetanus toxin (Tetx), a potent inhibitor of vesicle fusion via proteolysis of the requisite synaptic vesicle SNARE protein VAMP2 (Link et al., 1992). Tetx has been shown to block calcium-evoked dendritic exocytosis (Maletic-Savatic and Malinow, 1998), and attenuate AMPA receptor insertion into the postsynaptic membrane (Lu et al., 2001; Tatsukawa et al., 2006). Control neurons and Tetx-treated neurons were subjected to ratiometric calcium imaging using a two-pulse protocol of MO (Figures S4A,B and Figures 5E,F). The initial pulse of MO (30 μM, 2 min) was applied to determine MO-responsive (i.e. TRPA1-expressing) neurons and trigger surface translocation of TRPA1 (Figure 5E). Nine minutes later a second application of MO (150 μM, 2 min) was used to assess the levels of functional TRPA1 channels and therefore represented a read-out of TRPA1 sensitization [the higher concentration of MO in second pulse is to compensate for the expected desensitization of TRPA1 responses previously described (Hinman et al., 2006; Macpherson et al., 2007)]. The prediction is that Tetx-treated coverslips would exhibit a relatively reduced number of neurons responding to the second MO pulse if MO-induced increase in TRPA1 membrane levels is due to active exocytosis. Indeed, Tetx-treatment attenuated the second response to MO (Figure 5F). Importantly, Tetx had no significant effect on either the number of responders to the first pulse of MO (Figure 5E) or the amplitudes (Figures S4A,B) indicating that cultures were healthy and basal TRPA1 expression was not grossly altered by Tetx. These data suggest that activation of TRPA1 by MO induces active delivery and insertion of new channels into the membrane of sensory neurons, and, importantly, that a proportion of these channels are functional.

Vesicle-mediated fusion can also be investigated using voltage clamp techniques monitoring membrane capacitance (C_m) (Neher and Marty, 1982). We therefore examined whether MO could increase the membrane surface area of TRPA1-expressing DRG neurons. Previous reports on cultured DRG neurons have shown exocytosis to occur in response to depolarization (Huang and Neher, 1996). We reasoned that focal application of MO via the patch pipette might increase C_m in a TRPA1-dependent manner. We tested small to medium diameter neurons of wildtype and *Trpa1*-deficient (KO) cultures and monitored C_m of cell-attached patches of membrane for at least 5 minutes after sealing (Figures S5A,B). Forty percent of the patches from wildtype DRG exhibited specific changes in C_m with an average latency of 230 ± 50 sec (Figure 6A red bars**,** Figure 6B, wildtype). The rise in C_m required TRPA1, since comparable changes of C_m were not observed in *Trpa1*-deficient DRG neurons (Figure 6A and Figure S5B). Only 2 of 45 patches from *Trpa1*-deficient neurons revealed increases in surface area (Figure 6A, grey bars, inset), and the increases were significantly lower than those from wildtype patches (Figure 6B). The dependence on TRPA1 is not an artifact of the cells chosen to study (assessed by cell diameter) or electrode resistance, patch capacitance, or the ratio of series conductance to membrane conductance (G_s/G_m) since these parameters were not different between genotypes. Even though a few membrane patches revealed transient TRPA1-like conductance changes shortly after seal formation (n= 8 of 50) that were not observed in *Trpa1*-deficient neurons (n = 45), our recordings did not allow us to determine whether fusing vesicles contain TRPA1 channels (potentially due to desensitization of TRPA1 under these recording conditions and limited resolution of gating events). In summary, the capacitance recordings are in agreement with our previous data showing higher abundance of TRPA1 at the surface and involvement of vesicle-mediated fusion.

DISCUSSION

Preservation of sensitivity and sensitization of nociceptive neurons play an important role in acute and chronic pain transduction (Zhang and Bao, 2006). Numerous mechanisms including the release of inflammatory mediators and subsequent modulation of ion channels have been shown to be involved in these processes (Hucho and Levine, 2007; McMahon and Jones, 2004; Scholz and Woolf, 2002). This is the first study to investigate the cellular regulation of TRPA1, an ion channel with a unique mechanism of activation involved in transducing noxious signals. We generated specific antibodies against extracellular regions of murine TRPA1, which enabled selective visualization of surface-exposed TRPA1 channels in heterologous expression systems and primary sensory neurons. Our live-labeling experiments reveal increases in surface TRPA1 in response to seemingly different stimuli: pharmacological activators of protein kinase A (PKA) and phospholipase C (PLC), the TRPA1-specific agonist mustard oil (MO), as well as the TRPV1-specific agonist capsaicin. Importantly, our *in vitro* observations on the regulation of TRPA1 membrane levels correlate well with the effects of these stimuli on TRPA1 mediated responses *in vitro* and nocifensive behavior in animals. These data suggest that translocation of TRPA1 to the membrane is likely to be physiologically relevant *in vivo*, contributing to TRPA1 functionality and sensitization.

Many receptors and ion channels cycle between the plasma membrane and intracellular compartments, and the balance between membrane insertion and retrieval determines their surface abundance, and their activity (Ambudkar, 2007; Malenka, 2003; Shepherd and Huganir, 2007). Three observations reported here support the existence of such a regulation for TRPA1 channels: (i) PKA/PLC signaling, capsaicin, as well as activation of TRPA1 by MO enhance the availability of TRPA1 at the membrane in HEK cells and in sensory neurons. (ii) MO application to DRG neurons induced an increase of the membrane capacitance. This is indicative of incorporation of new membrane into the neuronal surface, which can be caused by membrane fusion-dependent events (Huang and Neher, 1996). (iii) Application of tetanus toxin selectively attenuated the response of cultured DRG to a second MO pulse. Taken

together, these data suggest that the increased TRPA1 membrane availability observed upon MO application is at least partially dependent on SNARE-mediated vesicle fusion. An interesting feature of this process is the lack of action of tetanus toxin on the initial MO response, which presumably reflects basal receptor levels. This may be indicative of tetanus toxin-independent/insensitive exocytosis at steady state, possibly involving different SNARE-proteins (Galli et al., 1998; Holt et al., 2008; Meng et al., 2007). Alternatively, incomplete proteolysis of VAMP2 by tetanus toxin might be sufficient to maintain constitutive TRPA1 insertion. On the other hand, MO-induced membrane translocation might require more rapid fusion events than at steady state and VAMP2 levels might become limiting. Similar findings are reported for activity-induced insertion and recycling of AMPA receptors (Lu et al., 2001; Tatsukawa et al., 2006). Collectively, our data suggest a translocation of functional TRPA1 channels to the membrane; however, we cannot exclude an attenuation of endocytotic events contributing to enhance surface labeling. One question, which has remained unsolved, is the identity of intracellular vesicles containing TRPA1 channels. New tools including more sensitive antibodies to TRPA1 will be required for future studies.

Interestingly, the MO-mediated increase in TRPA1 membrane expression can be attenuated by pharmacological blockade of PKA and PLC signaling. PKA and PLC activation, therefore, appear to be required downstream of TRPA1 activation and might provide a link between these two pathways. This notion is supported by previous studies showing TRPA1 activity upon PLC-dependent signaling in heterologous systems (Bandell et al., 2004). PLC activity affects cellular signaling by breakdown of phosphatidylinositides (PIP_2) into diacylglycerol (DAG) and inositol triphospate (IP3). While OAG, a membrane-permeable DAG analog, has been reported to activate TRPA1 (Bandell et al., 2004), the role of PIP_2 on TRPA1 is not settled. PIP_2 might promote TRPA1 activity (Akopian et al., 2007), but PIP_2-dependent inhibition of TRPA1 is also described (Dai et al., 2007). Further experiments are needed to determine the underlying mechanism and pathways of PLC-dependent TRPA1-sensitization. The possibility that PKA signaling and MO-induced TRPA1 activation might be linked is raised by a study on visceral pain induced by intracolonic injection of MO in rats (Wu et al., 2007). In this report, PKA activation appears to be a critical player in this pain model, as blockade of the PKA cascade partially reverses visceral pain-induced effects. However, unequivocal proof that PKA/PLC activation is crucial and a consequence of TRPA1 activation has not yet been demonstrated.

PKA and PLC are known instigators of inflammation and nociceptor sensitization, and their effects on cell signaling and neuronal inflammation can be diverse (Hucho and Levine, 2007). Many ion channels and receptors involved in pain signaling are phosphorylated by PKA, among them TRPV1 and the sodium channel $Na_V1.8$ (Bhave et al., 2002; Fitzgerald et al., 1999; Mohapatra and Nau, 2003). The phosphorylation status of receptors has been proposed to regulate channel activity and/or trafficking to the membrane (Esteban et al., 2003; Fabbretti et al., 2006; Zhang et al., 2005). In addition, PKA and PLC signaling cascades have been implicated in the regulation of vesicle-mediated fusion events (Holz and Axelrod, 2002; James et al., 2008; Seino and Shibasaki, 2005). In the context of TRPA1, PKA and PLC might be part of a multifactorial complex that controls surface expression of TRPA1. Future studies will investigate whether posttranslational modifications of TRPA1 and/or changes in the protein scaffold contribute to TRPA1 membrane expression. Furthermore, it will be of particular interest if similar mechanisms regulate TRPA1 membrane levels at the sensory nerve endings in the periphery, in agreement with what we observe in neuronal somata. The behavioral experiments showing sensitized TRPA1-mediated pain responses presented here suggest that this may be the case. To this end, sensitive tools for visualizing TRPA1 channels at sensory nerve endings in the plantar surface of mice hindpaws would have to be established.

Despite intensive study of TRPA1 and identification of a plethora of agonists, its molecular regulation and trafficking remain to be elucidated. Moreover, knowledge about these processes is key to understanding this important transduction channel in acute and inflammatory pain. The data presented here suggest that activation of sensory neurons via distinct but potentially linked mechanisms could enhance TRPA1 membrane insertion, resulting in higher amounts of functional TRPA1 channels at the surface. We propose that this process at least partly contributes to the regulation of nociceptor sensitivity to TRPA1 agonists.

EXPERIMENTAL PROCEDURES

Reagents

Mustard oil (MO), dimethyl sulfoxide (DMSO), N-(3-Trifluoromethylphenyl)-2,4,6 trimethylbenzenesulfonamide (m-3m3FBS), forskolin (FSK), tetanus toxin (Tetx), edelfosine (ET-18-OCH3) and N-[2-(p-Bromocinnamylamino)ethyl]-5-isoquinolinesulfonamide dihydrochloride (H89) were purchased from Sigma Aldrich (St. Louis, MO). Stock solutions were made as follows: MO and ET-18-OCH3 were dissolved in DMSO, Tetx in PBS, H89 in H_2O, FSK and m-3m3FBS in EtOH.

Generation of TRPA1 sera

Synthetic peptides were designed against extracellular domains of murine TRPA1 selected by using Kyte-Doolittle Hydrophilicity plots (Lasergene, DNAStar). Custom polyclonal antibodies to synthetic peptides TSSTHEERIDT (AbE1, in extracellular loop 1) and GDINYRDAFLEPLFRN (AbE3, in extracellular loop 3) were prepared in rabbit by standard methods and affinity purified (Imgenex Corp., San Diego, CA). Sera were dialyzed in PBS.

Behavior

All behavior analyses were conducted on 6 – 8 weeks old male C57Bl6 mice. Mice were acclimated for 20 min in a transparent plexiglass box at room temperature. Ten microliters of experimental agent (for more details see respective experiment in **RESULTS**) or of vehicle solution were injected subcutaneously into the plantar surface of the left hindpaw. Pain responses were measured by counting the time spent licking, flicking, or lifting the injected paw for 5 min. Seven to ten minutes later, mice were injected into the same position with ten microliters of the respective agents in solution (for more details see respective experiment in **RESULTS**). Acute pain was determined by measuring the time spent licking, flicking, or lifting the injected paw for 5 min after the second injection. All groups to be compared were assessed in parallel. All experiments were conducted with the approval of The Scripps Research Institute Animal Research Committee.

TRPA1 live-labeling and immunocytochemistry

Human embryonic kidney (HEK) 293T cells were maintained at 37 °C, 5 % CO_2 in DMEM containing 10 % FBS and antibiotic/antimycotic (Invitrogen). After transient transfection with 1.2 μg of a murine *Trpa1*-MYC/His construct (Macpherson et al., 2007) cells were plated on poly-D-lysine-coated glass bottom dishes (MatTek), which were additionally coated with laminin (2 μg/ml). Cells were used 18 – 24 hours after transfection. All groups to be compared were processed in parallel using the same culture preparation. Pharmacological agents were applied in culture medium at the concentrations and times indicated. For experiments under calcium-free conditions, pharmacological agents and TRPA1 antibodies were applied in calcium-free 1x Hanks' balanced salt solution (HBSS) (Invitrogen), 10 mM HEPES (Invitrogen), supplemented with 5 mM EGTA. H89, ET-O-CH18, FSK and m-3m3FBS were preincubated for 4 min before addition of MO or vehicle and were present throughout the incubation with the TRPA1 antibody. Surface TRPA1 was labeled by incubating live HEK

cells with TRPA1 antibodies (AbE1, 1:50) in pre-warmed culture medium for 10 min at 37 °C. Cells were washed 5 times with pre-warmed media and incubated with Alexa Fluor 488 F $(ab')_2$ fragment of goat-anti-rabbit (1:200, Invitrogen) for 10 min at room temperature. Cells were then washed 3 times in medium, once in PBS and fixed with 2 % PFA (paraformaldehyde in PBS) for 20 min at room temperature. Specificity of antibody-labeling was assessed by applying the same protocol to HEK cells expressing rat TRPV1 and by omission of the primary antibody. Neither control exhibited any label. Exclusive membrane staining with this protocol was tested using a brief acid wash [1 min, 0.5 M NaCl, 0.2 N acetic acid (Beattie et al., 2000)], which removed any live-labeling. In some cases cells were subjected to immunocytochemistry after PFA fixation. Cells were permeabilized in PBS containing 0.4 % Triton X-100, blocked with normal goat serum or normal donkey serum (10 % serum in PBS) and incubated with primary antibodies. The following primary antibodies were used: TRPV1 (1:50, goat, Santa Cruz Biotechnology); c-MYC (1:100, 9E11, mouse, Santa Cruz Biotechnology); wheat germ agglutinin Alexa Fluor 555 conjugate (1:200, Invitrogen). After three washes in PBS secondary antibodies were added. We used either Alexa Fluor 633 goat-anti-mouse IgG (1:200, Invitrogen,) or Alexa Fluor 568 donkey-anti-goat IgG (1:200, Invitrogen).

Endogenous TRPA1 channels in cultured DRG neurons were similarly labeled, but TRPA1 antibodies were diluted at 1:25. Cultured DRG from *Trpa1*-deficient animals (Kwan et al., 2006) stained the same way were devoid of staining and served as specificity control for TRPA1 antibodies. Preparation of DRG cultures is outlined in Supplemental Experimental Procedures.

Image acquisition and data analysis

TRPA1 live-labeling experiments in HEK cells were imaged at a Zeiss Axiovert 200 microscope (Carl Zeiss MicroImaging) using a 63x 1.4 NA PlanAPO oil-immersion objective, a Hamamatsu Orca-ER-II digital camera and MetaMorph software (Molecular Devices). Images for all experimental groups were taken using identical acquisition parameters. All groups to be compared were processed simultaneously using the same culture preparation. For each experimental group at least 10 cells were randomly analyzed from each preparation and experiments were done using at least 3 independent preparations. Raw images were analyzed using ImageJ software (ImageJ, NIH). The mean surface fluorescence intensity (AU) of each cell was determined by drawing a region of interest (ROI) carefully encircling the surface of each cell with the selection brush tool (pixel width 5). Values for background fluorescence for each individual cell were obtained by drawing a circular ROI exactly outside the cell surface. Mean background fluorescence intensity was then subtracted from the mean surface fluorescence intensity. These values were averaged among experiments.

TRPV1 surface levels were assessed in parallel with TRPA1 surface levels when both channels were coexpressed in HEK cells. TRPA1 live-label was used as a reference to delineate the membrane of each cell and determined as described above. The respective ROI of each cell was then transferred to TRPV1 images and the mean surface fluorescence intensity for TRPV1 was determined as described above for TRPA1.

TRPA1 live-labeling experiments on cultured DRG neurons were imaged at a Olympus (Tokyo, Japan) Fluoview 500 confocal microscope by sequential illumination using the 488 nm line of an argon laser, the HeNe green 543 nm laser and the HeNe red 633 nm laser. Merge stacked images were created using a 60x 1.4 NA PlanAPO oil-immersion objective. All groups to be compared were processed in parallel using the same DRG culture preparation (4 independent DRG preparations were used). The analysis of the mean fluorescence surface intensity was carried out on a single image plane from the middle of each stack as described above for HEK cells.

Capacitance recordings

DRG from wildtype or *Trpa1*-deficient mice (wildtype littermates gave similar results as colony C57Bl6) were recorded 18–48 hours after plating on poly-D-lysine/laminin coated coverslips. Cells were continuously perfused at 27–28 °C with 2 mM Ca^{2+} ES (in mM): 136 NaCl, 5 KCl, 2 $MgCl_2$, 2 $CaCl_2$, 10 dextrose and 10 HEPES, pH 7.4. Temperature was controlled with an in-line heater CL-100 (Warner Instruments). Patch pipettes were fabricated from B150-86 glass (Sutter Instrument Comp., Novaro, CA) and coated with Surgident Dental Periphery Wax (Heraeus, South Bend, IN). Pipette resistances were 0.7–2 MOhm when filled with 2 mM Ca^{2+} ES (tip) and backfilled with 2 mM Ca^{2+} ES containing 100 μM MO. Seals were made quickly (within a minute of backfilling) and capacitance (C_m) measurements were initiated immediately. Recordings were made using an EPC-9 patch clamp amplifier (HEKA Elektronic, InstruTECH Corp.,) with a built-in two-phase analog lock-in amplifier (Gillis, 2000; Lollike and Lindau, 1999). Admittance-based C_m measurements were performed using the “sine+dc” method using a 15 mV sine wave command voltage (Gillis, 2000; Lindau and Neher, 1988). Frequencies ranged from 1500 (67 μs, 15 kHz sampling rate) to 6000 Hz (14 μs, 71 kHz) to improve recordings (Debus and Lindau, 2000) and currents were filtered at 10 kHz and 30 kHz, respectively. Pipette holding potential was 0 mV. The continuous buffer was set to 14.2 M samples to enable prolonged recordings. C_m, G_m, and G_s components of the current recording were derived using a reversal potential of 60 mV. To avoid changes in C_m due to inadequate separation of C_m from G_m and G_s, data were included if calculated changes in C_m were not mirrored in G_m or G_s. While an early C_m change was observed in patches from both genotypes and may be due to effects arising from the sealing process, fluctuations that occurred at > 50 sec after sealing were very rarely observed in *Trpa1*-deficient DRG neurons. Average basal C_m for wildtype was 320 ± 20 fF and 340 ± 18 fF for *Trpa1*-deficient neurons, respectively. Exocytosis induced by a +120 mV step for 1 sec from separate cells of both genotypes served as a positive control for the ability to produce increases in C_m induced by a known stimulus of exocytosis in DRG neurons (Huang and Neher, 1996) and neuronal health (data not shown). While we cannot rule out a small contribution of membrane stretch to our capacitance measurements, the contribution would be relatively small based on theoretical and empirical considerations and cannot account for the observed changes. Even if the membrane were stretched through a TRPA1-dependent mechanism, energetic constraints limit changes in membrane thickness (and thus area) such that even the limiting stretch would produce a change in area of 1.85 % assuming no change in dielectric constant and constant volume of the membrane beneath the pipette (Hamill and Martinac, 2001). No visible cell swelling was observed over 10–15 min in the cell-attached patch configuration used here (data not shown).

Statistical analysis

If not stated otherwise, the nonparametric Mann-Whitney rank sum test was used for single comparisons and one-way ANOVA followed by Bonferroni’s multiple comparison test was used for multiple comparisons (GraphPad Prism software). All values refer to mean ± SEM; n indicates the sample number; P denotes the significance (* $P < 0.05$, ** $P < 0.01$, *** $P < 0.001$) and refers to the respective control (vehicle) in each experimental group if not noted otherwise; ns indicates “not significant”.

Supplementary Material

Refer to Web version on PubMed Central for supplementary material.

Acknowledgments

We thank Takashi Miyamoto for constructive suggestions and the members of the Patapoutian lab and David Gomez Varela for helpful discussions; Corinna Kimball and Dusko Trajkovic for technical assistance; Kathryn Spencer, for assistance with imaging; and Jorg Grandl and Anton Maximov, for critically reading the manuscript. We gratefully

acknowledge Dr. Wei Xiong and Dr. Bernd Letz (HEKA Elektronic) for providing technical expertise with capacitance recordings and Michael Caterina for providing rat *Trpv1* plasmid DNA. M.S. is supported by a postdoctoral fellowship from the German Academic Exchange Service (DAAD, D/07/41089). This research was supported by NIH R01 grants NS049104-04 and NS046303-06.

References

Akopian AN, Ruparel NB, Jeske NA, Hargreaves KM. Transient receptor potential TRPA1 channel desensitization in sensory neurons is agonist dependent and regulated by TRPV1-directed internalization. The Journal of physiology 2007;583:175–193. [PubMed: 17584831]

Ambudkar IS. Trafficking of TRP channels: determinants of channel function. Handbook of experimental pharmacology 2007:541–557. [PubMed: 17217078]

Bandell M, Story GM, Hwang SW, Viswanath V, Eid SR, Petrus MJ, Earley TJ, Patapoutian A. Noxious cold ion channel TRPA1 is activated by pungent compounds and bradykinin. Neuron 2004;41:849–857. [PubMed: 15046718]

Bao L, Jin SX, Zhang C, Wang LH, Xu ZZ, Zhang FX, Wang LC, Ning FS, Cai HJ, Guan JS, et al. Activation of delta opioid receptors induces receptor insertion and neuropeptide secretion. Neuron 2003;37:121–133. [PubMed: 12526778]

Bautista DM, Jordt SE, Nikai T, Tsuruda PR, Read AJ, Poblete J, Yamoah EN, Basbaum AI, Julius D. TRPA1 mediates the inflammatory actions of environmental irritants and proalgesic agents. Cell 2006;124:1269–1282. [PubMed: 16564016]

Bautista DM, Movahed P, Hinman A, Axelsson HE, Sterner O, Hogestatt ED, Julius D, Jordt SE, Zygmunt PM. Pungent products from garlic activate the sensory ion channel TRPA1. Proceedings of the National Academy of Sciences of the United States of America 2005;102:12248–12252. [PubMed: 16103371]

Beattie EC, Carroll RC, Yu X, Morishita W, Yasuda H, von Zastrow M, Malenka RC. Regulation of AMPA receptor endocytosis by a signaling mechanism shared with LTD. Nature neuroscience 2000;3:1291–1300.

Bhave G, Zhu W, Wang H, Brasier DJ, Oxford GS, Gereau RWt. cAMP-dependent protein kinase regulates desensitization of the capsaicin receptor (VR1) by direct phosphorylation. Neuron 2002;35:721–731. [PubMed: 12194871]

Conaway CC, Krzeminski J, Amin S, Chung FL. Decomposition rates of isothiocyanate conjugates determine their activity as inhibitors of cytochrome p450 enzymes. Chemical research in toxicology 2001;14:1170–1176. [PubMed: 11559030]

Dai Y, Wang S, Tominaga M, Yamamoto S, Fukuoka T, Higashi T, Kobayashi K, Obata K, Yamanaka H, Noguchi K. Sensitization of TRPA1 by PAR2 contributes to the sensation of inflammatory pain. The Journal of clinical investigation 2007;117:1979–1987. [PubMed: 17571167]

Debus K, Lindau M. Resolution of patch capacitance recordings and of fusion pore conductances in small vesicles. Biophysical journal 2000;78:2983–2997. [PubMed: 10827977]

Diogenes A, Akopian AN, Hargreaves KM. NGF up-regulates TRPA1: implications for orofacial pain. Journal of dental research 2007;86:550–555. [PubMed: 17525356]

Esteban JA, Shi SH, Wilson C, Nuriya M, Huganir RL, Malinow R. PKA phosphorylation of AMPA receptor subunits controls synaptic trafficking underlying plasticity. Nature neuroscience 2003;6:136–143.

Fabbretti E, D'Arco M, Fabbro A, Simonetti M, Nistri A, Giniatullin R. Delayed upregulation of ATP P2X3 receptors of trigeminal sensory neurons by calcitonin gene-related peptide. J Neurosci 2006;26:6163–6171. [PubMed: 16763024]

Fitzgerald EM, Okuse K, Wood JN, Dolphin AC, Moss SJ. cAMP-dependent phosphorylation of the tetrodotoxin-resistant voltage-dependent sodium channel SNS. The Journal of physiology 1999;516 (Pt 2):433–446. [PubMed: 10087343]

Galli T, Zahraoui A, Vaidyanathan VV, Raposo G, Tian JM, Karin M, Niemann H, Louvard D. A novel tetanus neurotoxin-insensitive vesicle-associated membrane protein in SNARE complexes of the apical plasma membrane of epithelial cells. Molecular biology of the cell 1998;9:1437–1448. [PubMed: 9614185]

Gillis KD. Admittance-based measurement of membrane capacitance using the EPC-9 patch-clamp amplifier. Pflugers Arch 2000;439:655–664. [PubMed: 10764227]

Hamill OP, Martinac B. Molecular basis of mechanotransduction in living cells. Physiological reviews 2001;81:685–740. [PubMed: 11274342]

Hinman A, Chuang HH, Bautista DM, Julius D. TRP channel activation by reversible covalent modification. Proceedings of the National Academy of Sciences of the United States of America 2006;103:19564–19568. [PubMed: 17164327]

Holt M, Riedel D, Stein A, Schuette C, Jahn R. Synaptic vesicles are constitutively active fusion machines that function independently of Ca2+ Curr Biol 2008;18:715–722. [PubMed: 18485705]

Holz RW, Axelrod D. Localization of phosphatidylinositol 4,5-P(2) important in exocytosis and a quantitative analysis of chromaffin granule motion adjacent to the plasma membrane. Annals of the New York Academy of Sciences 2002;971:232–243. [PubMed: 12438123]

Huang LY, Neher E. Ca(2+)-dependent exocytosis in the somata of dorsal root ganglion neurons. Neuron 1996;17:135–145. [PubMed: 8755485]

Hucho T, Levine JD. Signaling pathways in sensitization: toward a nociceptor cell biology. Neuron 2007;55:365–376. [PubMed: 17678851]

James DJ, Khodthong C, Kowalchyk JA, Martin TF. Phosphatidylinositol 4,5-bisphosphate regulates SNARE-dependent membrane fusion. The Journal of cell biology 2008;182:355–366. [PubMed: 18644890]

Ji G, Zhou S, Carlton SM. Intact Adelta-fibers up-regulate transient receptor potential A1 and contribute to cold hypersensitivity in neuropathic rats. Neuroscience 2008;154:1054–1066. [PubMed: 18514429]

Ji RR, Samad TA, Jin SX, Schmoll R, Woolf CJ. p38 MAPK activation by NGF in primary sensory neurons after inflammation increases TRPV1 levels and maintains heat hyperalgesia. Neuron 2002;36:57–68. [PubMed: 12367506]

Katsura H, Obata K, Mizushima T, Yamanaka H, Kobayashi K, Dai Y, Fukuoka T, Tokunaga A, Sakagami M, Noguchi K. Antisense knock down of TRPA1, but not TRPM8, alleviates cold hyperalgesia after spinal nerve ligation in rats. Experimental neurology 2006;200:112–123. [PubMed: 16546170]

Kwan KY, Allchorne AJ, Vollrath MA, Christensen AP, Zhang DS, Woolf CJ, Corey DP. TRPA1 contributes to cold, mechanical, and chemical nociception but is not essential for hair-cell transduction. Neuron 2006;50:277–289. [PubMed: 16630838]

Lindau M, Neher E. Patch-clamp techniques for time-resolved capacitance measurements in single cells. Pflugers Arch 1988;411:137–146. [PubMed: 3357753]

Link E, Edelmann L, Chou JH, Binz T, Yamasaki S, Eisel U, Baumert M, Sudhof TC, Niemann H, Jahn R. Tetanus toxin action: inhibition of neurotransmitter release linked to synaptobrevin proteolysis. Biochemical and biophysical research communications 1992;189:1017–1023. [PubMed: 1361727]

Lollike K, Lindau M. Membrane capacitance techniques to monitor granule exocytosis in neutrophils. Journal of immunological methods 1999;232:111–120. [PubMed: 10618513]

Lu W, Man H, Ju W, Trimble WS, MacDonald JF, Wang YT. Activation of synaptic NMDA receptors induces membrane insertion of new AMPA receptors and LTP in cultured hippocampal neurons. Neuron 2001;29:243–254. [PubMed: 11182095]

Macpherson LJ, Dubin AE, Evans MJ, Marr F, Schultz PG, Cravatt BF, Patapoutian A. Noxious compounds activate TRPA1 ion channels through covalent modification of cysteines. Nature 2007;445:541–545. [PubMed: 17237762]

Malenka RC. Synaptic plasticity and AMPA receptor trafficking. Annals of the New York Academy of Sciences 2003;1003:1–11. [PubMed: 14684431]

Maletic-Savatic M, Malinow R. Calcium-evoked dendritic exocytosis in cultured hippocampal neurons. Part I: trans-Golgi network-derived organelles undergo regulated exocytosis. J Neurosci 1998;18:6803–6813. [PubMed: 9712651]

McMahon SB, Jones NG. Plasticity of pain signaling: role of neurotrophic factors exemplified by acid-induced pain. Journal of neurobiology 2004;61:72–87. [PubMed: 15362154]

Meng J, Wang J, Lawrence G, Dolly JO. Synaptobrevin I mediates exocytosis of CGRP from sensory neurons and inhibition by botulinum toxins reflects their anti-nociceptive potential. Journal of cell science 2007;120:2864–2874. [PubMed: 17666428]

Mohapatra DP, Nau C. Desensitization of capsaicin-activated currents in the vanilloid receptor TRPV1 is decreased by the cyclic AMP-dependent protein kinase pathway. The Journal of biological chemistry 2003;278:50080–50090. [PubMed: 14506258]

Nagata K, Duggan A, Kumar G, Garcia-Anoveros J. Nociceptor and hair cell transducer properties of TRPA1, a channel for pain and hearing. J Neurosci 2005;25:4052–4061. [PubMed: 15843607]

Neher E, Marty A. Discrete changes of cell membrane capacitance observed under conditions of enhanced secretion in bovine adrenal chromaffin cells. Proceedings of the National Academy of Sciences of the United States of America 1982;79:6712–6716. [PubMed: 6959149]

Obata K, Katsura H, Mizushima T, Yamanaka H, Kobayashi K, Dai Y, Fukuoka T, Tokunaga A, Tominaga M, Noguchi K. TRPA1 induced in sensory neurons contributes to cold hyperalgesia after inflammation and nerve injury. The Journal of clinical investigation 2005;115:2393–2401. [PubMed: 16110328]

Oheim M, Kirchhoff F, Stuhmer W. Calcium microdomains in regulated exocytosis. Cell calcium 2006;40:423–439. [PubMed: 17067670]

Ruparel NB, Patwardhan AM, Akopian AN, Hargreaves KM. Homologous and heterologous desensitization of capsaicin and mustard oil responses utilize different cellular pathways in nociceptors. Pain 2008;135:271–279. [PubMed: 17590514]

Scholz J, Woolf CJ. Can we conquer pain? Nature neuroscience 2002;5(Suppl):1062–1067.

Seino S, Shibasaki T. PKA-dependent and PKA-independent pathways for cAMP-regulated exocytosis. Physiological reviews 2005;85:1303–1342. [PubMed: 16183914]

Shepherd JD, Huganir RL. The cell biology of synaptic plasticity: AMPA receptor trafficking. Annual review of cell and developmental biology 2007;23:613–643.

Story GM, Peier AM, Reeve AJ, Eid SR, Mosbacher J, Hricik TR, Earley TJ, Hergarden AC, Andersson DA, Hwang SW, et al. ANKTM1, a TRP-like channel expressed in nociceptive neurons, is activated by cold temperatures. Cell 2003;112:819–829. [PubMed: 12654248]

Tappe-Theodor A, Agarwal N, Katona I, Rubino T, Martini L, Swiercz J, Mackie K, Monyer H, Parolaro D, Whistler J, et al. A molecular basis of analgesic tolerance to cannabinoids. J Neurosci 2007;27:4165–4177. [PubMed: 17428994]

Tatsukawa T, Chimura T, Miyakawa H, Yamaguchi K. Involvement of basal protein kinase C and extracellular signal-regulated kinase 1/2 activities in constitutive internalization of AMPA receptors in cerebellar Purkinje cells. J Neurosci 2006;26:4820–4825. [PubMed: 16672655]

Wang S, Dai Y, Fukuoka T, Yamanaka H, Kobayashi K, Obata K, Cui X, Tominaga M, Noguchi K. Phospholipase C and protein kinase A mediate bradykinin sensitization of TRPA1: a molecular mechanism of inflammatory pain. Brain 2008a;131:1241–1251. [PubMed: 18356188]

Wang YY, Chang RB, Waters HN, McKemy DD, Liman ER. The nociceptor ion channel TRPA1 is potentiated and inactivated by permeating calcium ions. J Biol Chem 2008b;283:32691–32703. [PubMed: 18775987]

Wu J, Su G, Ma L, Zhang X, Lei Y, Lin Q, Nauta HJ, Li J, Fang L. The role of c-AMP-dependent protein kinase in spinal cord and post synaptic dorsal column neurons in a rat model of visceral pain. Neurochemistry international 2007;50:710–718. [PubMed: 17320244]

Zhang X, Bao L. The development and modulation of nociceptive circuitry. Current opinion in neurobiology 2006;16:460–466. [PubMed: 16828278]

Zhang X, Bao L, Guan JS. Role of delivery and trafficking of delta-opioid peptide receptors in opioid analgesia and tolerance. Trends in pharmacological sciences 2006;27:324–329. [PubMed: 16678916]

Zhang X, Huang J, McNaughton PA. NGF rapidly increases membrane expression of TRPV1 heat-gated ion channels. The EMBO journal 2005;24:4211–4223. [PubMed: 16319926]

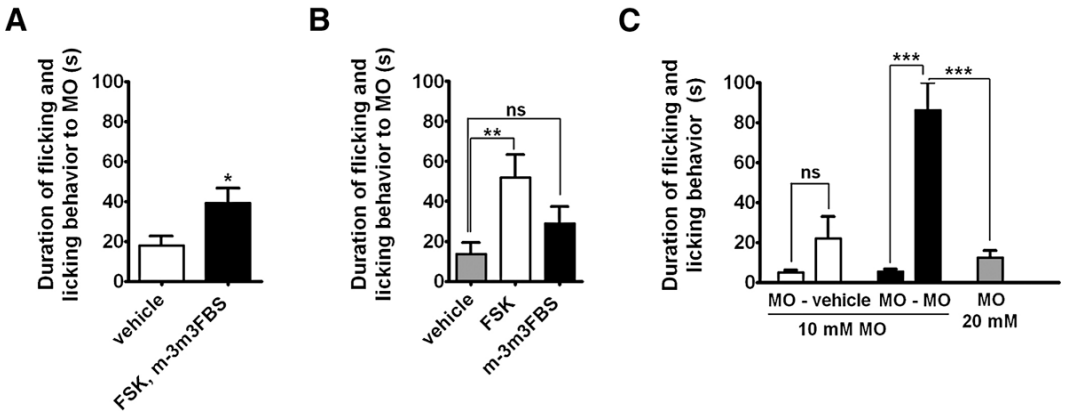

Figure 1. TRPA1-mediated pain responses can be sensitized *in vivo*

(A) C57Bl6 male mice were injected with vehicle (12 % EtOH) or FSK, m-3m3FBS (1 mM each) followed by an injection of MO (1 mM). Plots show quantitation of the response duration of acute nocifensive behavior to MO during 5 minutes after vehicle (18.0 ± 4.7 s) and FSK, m-3m3FBS (39.1 ± 7.5 s) pre-injection in the paw (n = 12 mice for vehicle and n = 11 mice for FSK, m-3m3FBS). P = 0.0338, Mann-Whitney test. **(B)** C57Bl6 male mice were injected with vehicle (12 % EtOH), FSK (6 mM) or m-3m3FBS (1.2 mM) followed by an injection of MO (1 mM). Plots show quantitation of the response duration of acute nocifensive behavior to MO during 5 minutes after vehicle (13.6 ± 5.7 s), FSK (51.9 ± 11.4 s) or m-3m3FBS (28.8 ± 8.7 s) pre-injection in the paw (n = 12 mice for each condition). FSK sensitizes TRPA1-mediated responses compared to vehicle. ** $P < 0.01$; one-way ANOVA followed by Dunnett's Multiple Comparison Test. **(C)** C57Bl6 male mice were injected with MO (10 mM), and the duration of acute nocifensive behavior was measured for each group for 5 min (5.0 ± 1.3 s and 5.6 ± 1.2 s; n = 8 mice for each group). Subsequently mice were either injected with MO (10 mM) or vehicle (1 % DMSO in PBS) and again, acute nocifensive behavior was assessed for 5 min. Plots show quantitation of the response duration to either injection (n = 8 mice for each group). Responses to a second MO injection (86.1 ± 13.8 s) were significantly enhanced compared to vehicle injection (22.0 ± 11.0 s) or single injection of 20 mM MO (12.6 ± 3.5 s; n = 8 mice). *** $P < 0.001$, one-way ANOVA followed by Bonferroni's multiple comparison test.

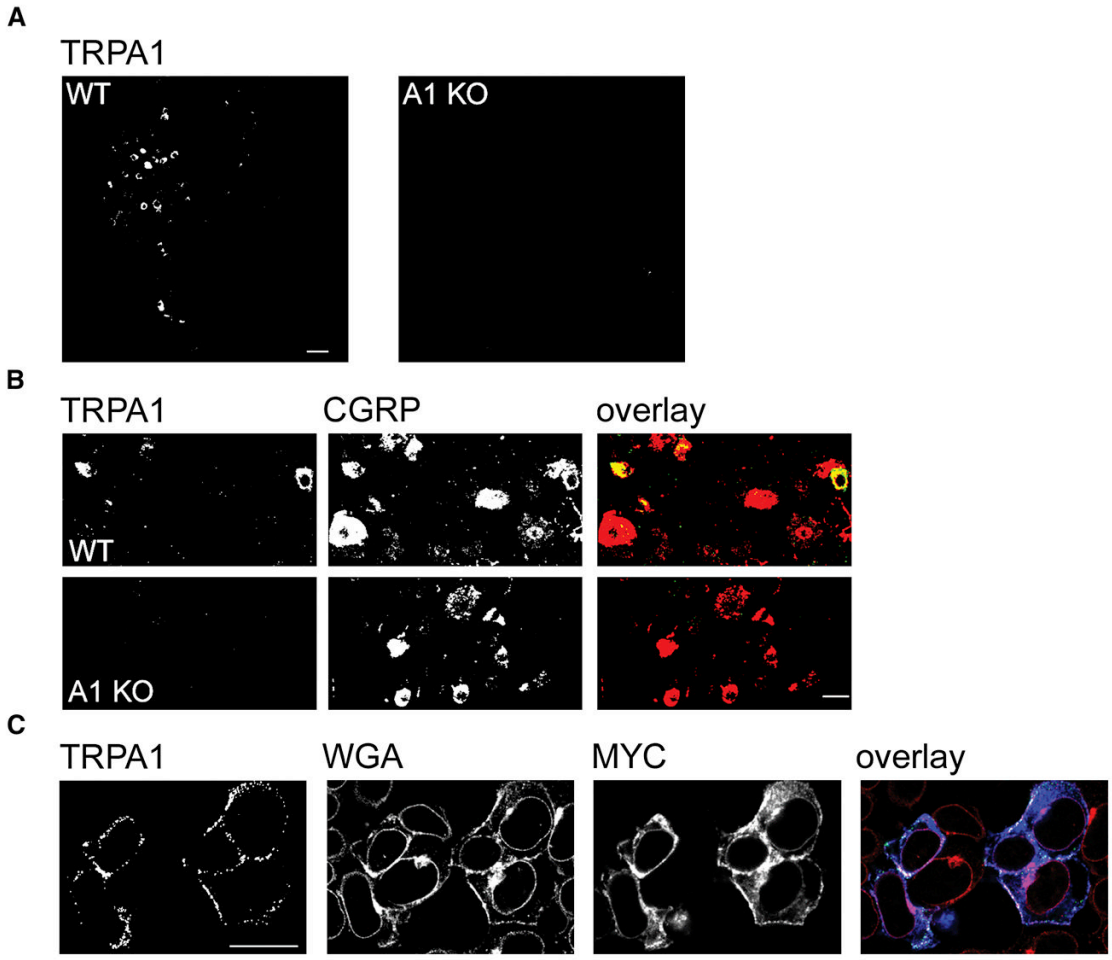

Figure 2. Specificity of TRPA1 antibodies

(A) Cryosections of wildtype (WT) adult trigeminal (TG) neurons (left) show staining for TRPA1 whereas TG neurons of *Trpa1*-deficient animals (A1 KO, right) are devoid of staining. Scale bar = 50 μm. **(B)** TRPA1-positive TG express the nociceptive marker CGRP (upper panel). TG from *Trpa1*-deficient animals (A1 KO) exhibit CGRP staining (lower panel), but are devoid of TRPA1 staining. Scale bar = 30 μm **(C)** Heterologous expression of TRPA1-MYC in HEK cells. Cells were live-labeled with TRPA1 antibodies (AbE1, green), fixed, permeabilized and stained for WGA (red) and MYC (blue). Only cells exhibiting MYC labeling are detected by TRPA1 antibodies. TRPA1 labeling is restricted to the cell surface as indicated by comparison with the staining pattern of WGA. Scale bar = 20 μm

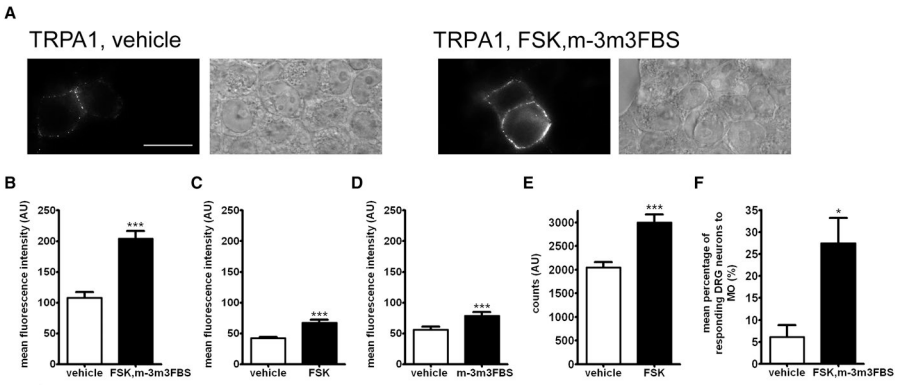

Figure 3. The intensity of TRPA1 membrane staining and functionality is modulated by PKA and PLC signaling

(A) Representative images of live-labeling of surface TRPA1 channels and bright field images of the respective field of view after application of vehicle (EtOH) and FSK, m-3m3FBS (30 μM and 25 μM, respectively) to TRPA1-expressing HEK cells. Scale bar = 20 μm **(B)** Quantitation of the mean fluorescence intensity of TRPA1 labeling in vehicle (n = 51) and FSK, m-3m3FBS -treated cells (n = 64). **(C)** Quantitation of the mean fluorescence intensity of TRPA1 labeling in vehicle (n = 124) and FSK - treated cells (100 μM; n = 123). **(D)** Quantitation of the mean fluorescence intensity of TRPA1 labeling in vehicle (n = 83) compared to m-3m3FBS - treated cells (60 μM; n = 82). **(E)** FLIPR-based calcium imaging of TRPA1-expressing HEK cells. Cells were incubated with FSK (100 μM) or vehicle followed by addition of MO (0.3 μM). Quantitation of the mean amplitude of TRPA1-mediated calcium influx upon pre-treatment with vehicle (n = 16 wells, 8000 cells/well) and FSK (n = 16 wells, 8000 cells/well). **(F)** Ratiometric calcium imaging of cultured DRG neurons. Neurons were incubated with FSK (100 μM) and m-3m3FBS (50 μM) or vehicle followed by addition of MO (5 μM). Quantitation of the mean percentage of responding DRG neurons upon pretreatment with vehicle (6.1 ± 2.8 %, n = 720 neurons) and FSK, m-3m3FBS (27.42 ± 5.8 %, n = 480 neurons). P = 0.019.

* P < 0.05, *** P < 0.001, Mann-Whitney test.

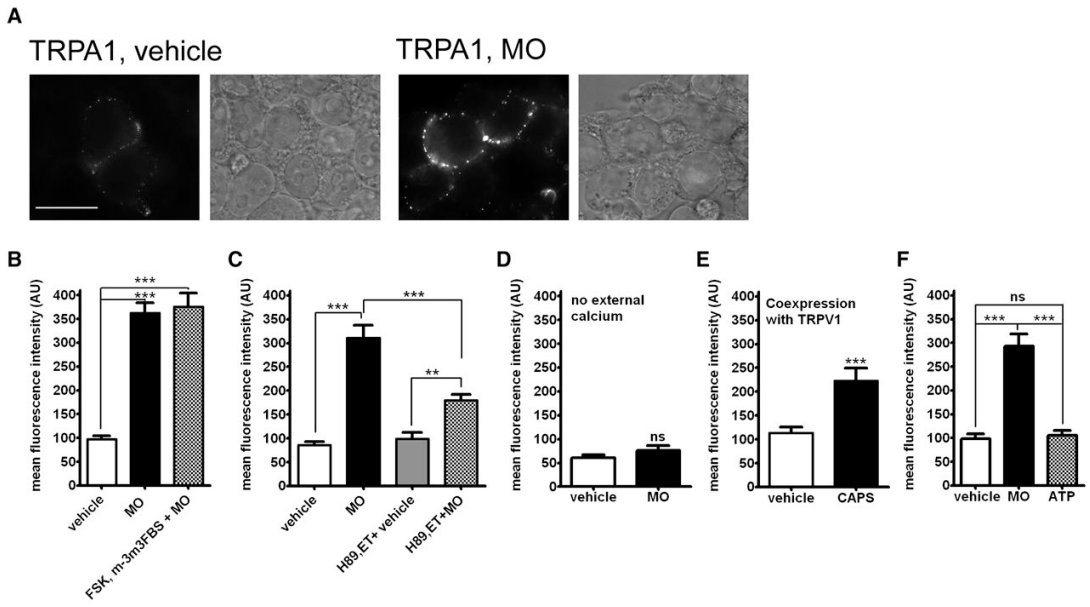

Figure 4. MO-induced activation of TRPA1 increases TRPA1 surface labeling

(A) Representative images of live-labeling of surface TRPA1 channels and bright field images of the respective field of view after application of vehicle (DMSO) and and MO (100 μM, 1 min) to TRPA1-expressing HEK cells. Scale bar = 20 μm **(B)** Quantitation of the mean fluorescence intensity of TRPA1 labeling in vehicle-treated (n = 72), MO-treated (n = 75), and MO-treated cells preincubated with FSK, m-3m3FBS (30 μM and 25 μM, respectively; n = 34). **(C)** MO-dependent increase of TRPA1 surface levels can be attenuated by blockade of PKA- and PLC-signaling by application of H89 (20 μM) and ET (10 μM). Quantitation of the mean fluorescence intensity of TRPA1 surface labeling in vehicle-treated (n = 51) versus MO-treated (n = 42) cells compared to the same treatments in the presence of H89 and ET (vehicle n = 34; MO n = 60). **(D)** MO-dependent increase of TRPA1 surface labeling is abolished in the absence of extracellular calcium (vehicle n = 35; MO n = 43). **(E)** Co-expression of TRPA1 and TRPV1. Quantitation of the mean fluorescence intensity of TRPA1 membrane labeling upon application of CAPS (1 min, 1 μM, n = 46) and vehicle (DMSO, n = 43). *** $P < 0.001$, Mann-Whitney test. **(F)** Quantitation of the mean fluorescence intensity of TRPA1 labeling in cells treated with vehicle (n = 38), MO (n = 44) and ATP (100 μM, 1 min; n = 48).
** $P < 0.01$, *** $P < 0.001$, one-way ANOVA followed by Bonferroni's multiple comparison test.

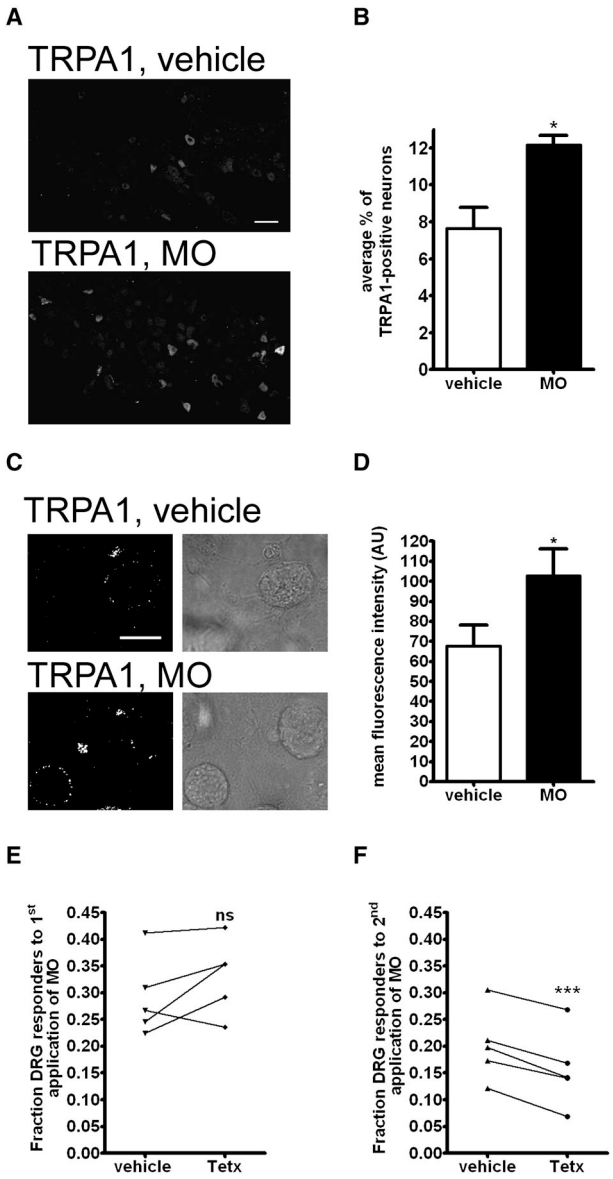

Figure 5. Activation of TRPA1 by MO acutely affects the abundance of observed endogenous TRPA1 channels

(A) Explants of trigeminal ganglia were incubated with vehicle (DMSO) or MO (100 μM, 15 min), immediately fixed, and cryosections were stained with TRPA1-antibodies. Scale bar = 50 μm **(B)** Quantitation of the average percentage of TRPA1-positive neurons upon vehicle (7.7 ± 1.1 %; n = 3516 neurons) and MO (12.2 ± 0.5 %; n = 4548 neurons) application (n = 4 animals). P = 0.028, Mann-Whitney test. **(C)** Representative raw images of live-labeling of endogenous TRPA1 in cultured DRG neurons after application of vehicle and MO (100 μM, 1 min), respectively. Scale bar = 20 μm **(D)** Quantitation of the mean fluorescence intensity of TRPA1 surface labeling in neurons incubated with vehicle (n = 23) and MO (n = 25). P = 0.028, Mann-Whitney test. **(E,F)** Ratiometric calcium imaging in cultured DRG from wildtype mice (vehicle: n = 206 neurons/animal; Tetx: n = 280 neurons/animal; n = 5 animals). **(E)** Paired analysis of the fraction of DRG neurons responding to the first pulse of MO in presence of vehicle (29.2 ± 3.3%;) and tetanus toxin (Tetx; 33.1 ± 3.2%), respectively. **(F)** Paired analysis

of the fraction of DRG neurons responding to the second pulse of MO in presence of vehicle (20.2 ± 3.0%) and tetanus toxin (Tetx; 15.8 ± 3.2%), respectively. P = 0.0005 paired Student's *t*-test.

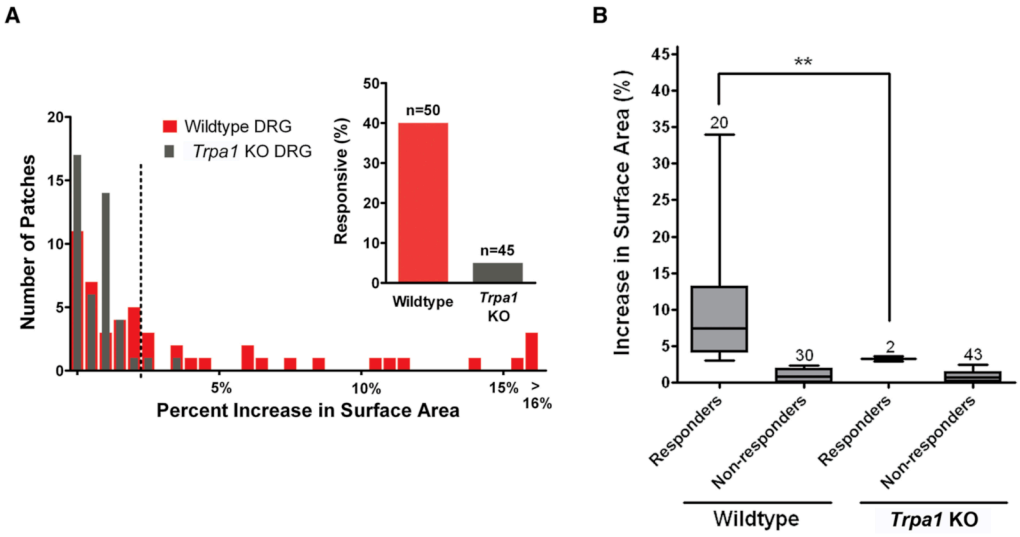

Figure 6. MO causes an increase in cell-attached patch membrane capacitance in wildtype, but not *Trpa1*-deficient (KO) small diameter sensory neurons

(A) Histogram of the percent increase of surface area observed in wildtype (red) and *Trpa1* KO (grey) neurons. Dashed line indicates two times the standard deviation of the average increase in surface area observed for patches from *Trpa1*-deficient cells. Responding patches are those with changes in surface area > 2.5 %. Inset: The percent responders for wildtype and *Trpa1* KO neurons of the total number of cells tested (n). P < 3e-6; ChiSquare. **(B)** Box plots of the percent increase in surface area for responders (10.9 ± 2.1%, n = 20) of the surface area of the patch and non-responders (n = 30) from cultures derived from wildtype and *Trpa1* KO mice (total n = 45). The two outlier *Trpa1* KO responding cells are well below the lower quartile of the wildtype responders. P < 0.002, Student's *t*-test.